Vortex capturing vertical axis wind turbine

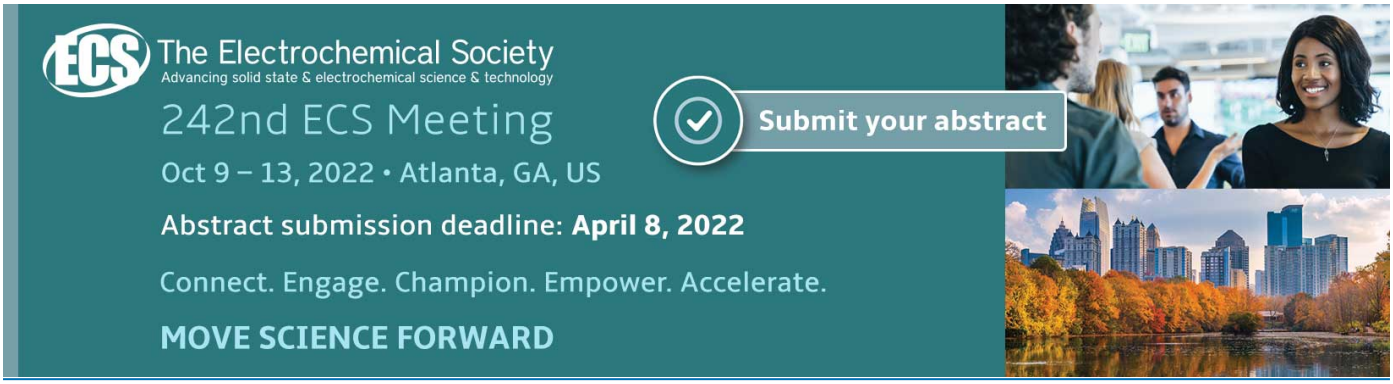

Journal of Physics: Conference Series **75** (2007) 012029 doi:10.1088/1742-6596/75/1/012029

Vortex capturing vertical axis wind turbine

L Zannetti, F Gallizio and G Ottino

Dept. of Aerospace Engineering, Politecnico di Torino, Turin, Italy

E-mail: luca.zannetti@polito.it, federico.gallizio@polito.it, gabriele.ottino@polito.it

Abstract. An analytical-numerical study is presented for an innovative lift vertical axis turbine whose blades are designed with vortex trapping cavities that act as passive flow control devices. The unsteady flow field past one-bladed and two-bladed turbines is described by a combined analytical and numerical method based on conformal mapping and on a blob vortex method.

1. Introduction

The paper is devoted to the study of innovative small/medium size wind or hydraulic vertical axis turbines (VAT).

The proposed VAT architecture is a variation of the Darrieus turbine, which in general consists of a couple of curved or straight blades rotating around a vertical shaft. The main problem with the Darrieus architecture is the complicated unsteady flow phenomena occurring during its working cycle. During each revolution, the blades of traditional Darrieus turbines undergo a highly unsteady relative fluid motion with large oscillation of the incidence. Dynamic stall can occur and the consequent uncontrolled flow detachment and vortex shedding result in high drag and low efficiency.

Recent developments offer a tool to design blades with innovative vortex trapping cavities that act as a passive control device capable of avoiding the vortex shedding, thus enhancing the efficiency. A research European project on this subject is in progress (see [7]). Such devices are mainly investigated to control the stall of aircraft wings. In general, vortex trapping is a technology for preventing vortex shedding and reducing the drag in the flow past bluff bodies. The concept is old (see, for instance, [1]). Some experience on studying airfoils with cavities has been already gained, see for instance [2],[3],[4],[5],[6].

Here we extend such ideas to unconventional lift VATs. Since the incidence oscillates between opposite values, the traditional design consists of symmetric blade sections which operate poorly at high angles of attack. The performance of the turbine can be improved by exploiting the capability of properly designed cavities to stabilize the flow by trapping a vortex. A blade profile with cavities is shown in fig. 1. The flow past the profile is forced to separate on the edge, vortices are trapped by the cavity and reattachment occurs on the smooth end of the cavity. At stall condition, the erratic unsteadiness of the separation points is avoided and the flow structure with trapped vortices is preserved. Moreover, since at incidence the trapped vortices are not symmetric, the airfoil acts as an adaptive airfoil that changes its camber in favour of the incoming flow.

In the present study, the flow is assumed as incompressible and inviscid, with the shed vorticity modelled by vortex singularities. Conformal mapping and a vortex method are the tools used to describe the evolution of the unsteady flow field. An exhaustive discussion about the advantage of this procedure with respect to alternative approaches, as distributed singularity methods, is presented in [8].

The paper organization is the following: Sec. 2 illustrates the method to solve the flow field past a one-bladed turbine together with some numerical results. In Sec. 3 the study is extended to two-bladed turbines. The evaluation of the turbine performances are discussed in Sec. 4 and concluding remarks are presented in Sec. 5.

2. Single blade turbine

Firstly consider the flow past a turbine with a single blade having three sharp edges, as shown in fig 1. Due to the unsteadiness of the motion, the circulation past the airfoil varies in time and, as a consequence, vorticity is shed by the profile. Neglecting secondary separations, the vorticity is shed by the sharp edges of the airfoil, with the T_1 and T_2 edges generating two vortical structures trapped by the cavities and with the T_e edge generating a wake.
The flow is modelled as a potential flow with vortex singularities representing the vorticity shed by the sharp edges of the blade.

According to the Riemann mapping theorem, the blade can be conformally mapped from the physical complex z-plane onto the unit circle of the transformed complex ζ-plane by an analytical function $\zeta = \zeta(z)$ where $\lim_{z\to\infty} \zeta = \infty$. The complex potential $w_\zeta = w_\zeta(\zeta)$ is determined on the transformed ζ-plane as described below. Exploiting its invariance under conformal mapping, the complex potential on the physical z-plane is then $w(z) = w(\zeta(z))$.

For an arbitrary blade section, the mapping can be performed as a chain of transformations. Following Moretti [9], firstly the airfoil section is mapped onto a quasi-circular figure of an intermediate plane by smoothing the sharp edges by means of a sequence of Kármán-Trefftz transformations, then the Theodorsen-Garrick transformation can be used to bring the quasi-circle onto the unit circle of the final transformed ζ-plane. The last step can be conveniently done following the iterative process described by Ives [10]. The $z = z(\zeta)$ transformation from the unit circle of the ζ-plane to the physical z-plane is obtained by inverting the mapping sequence.

The purpose of the present work is to show, in principle, the working mechanism of a blade with trapping vortex cavities. To simplify and speed up the flow computation, it has been devised a $z = z(\zeta)$ function that maps the unit circle of the ζ-plane directly onto an airfoil with two cavities of the z-plane. The generated blade section results in a variation of a Kármán-Trefftz profile. By so doing, the mapping is defined by simple analytic functions in closed form and the time consuming evaluations of the series involved by the Theodorsen-Garrick mapping are avoided by the flow computation.

The mapping chain is shown in fig. 1. The unit circle of the ζ-plane is mapped onto the intermediate λ-plane by

$$\lambda = \zeta + \frac{a}{\zeta - \zeta_1} + \frac{b}{\zeta - \zeta_2}.$$

where ζ_1, ζ_2 are points inside the unit circle and a, b are such that$(d\lambda/d\zeta)_{\zeta_{T_1}} = (d\lambda/d\zeta)_{\zeta_{T_2}} = 0$, with ζ_{T_1}, ζ_{T_2} being the images on the circle of the cusped edges of the cavities. The point $\zeta_{T_e} = 1$ is the image of the airfoil trailing edge. The airfoil is generated on the z-plane by the Kármán-Trefftz mapping

$$\frac{z-1}{z+1} = \left(\frac{\lambda - \lambda_{T_e}}{\lambda - \lambda_N}\right)^\tau, \qquad \tau = 2 - \epsilon/\pi,$$

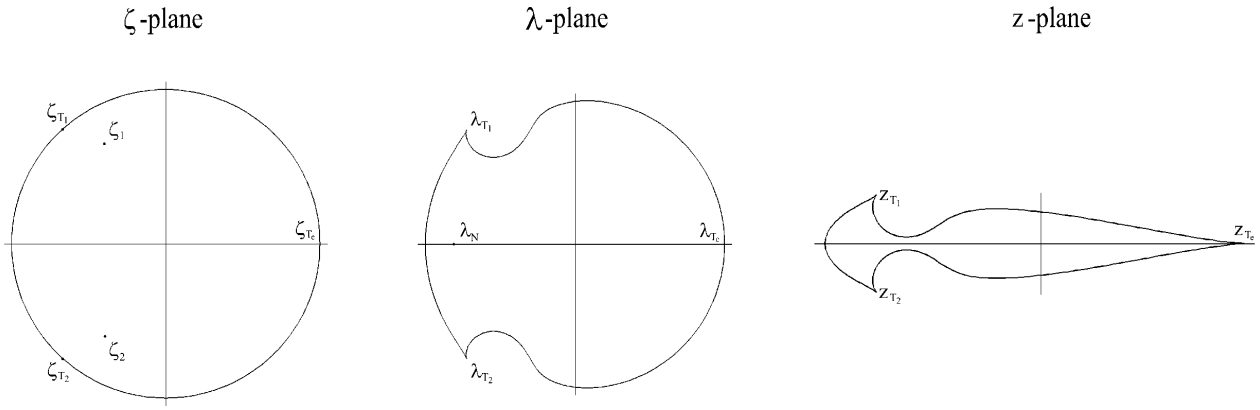

Figure 1. Mapping sequence for a one-bladed turbine. $\zeta_1 = \bar{\zeta}_2 = -.463 + .807i$, $\zeta_{T_1} = \bar{\zeta}_{T_2} = -.602 + .799i$.

with ϵ being the trailing edge angle. As shown in fig. 1, λ_{T_e} corresponds to the trailing edge while λ_N corresponds to a point inside the airfoil and close to its nose.

The mapping depends on the choice of the parameters $\zeta_1, \zeta_2, \zeta_{T_1}, \zeta_{T_2}, \lambda_N, \epsilon$, that is, it depends on eleven real parameters. For symmetric airfoils, as here considered, the real parameters reduce to six, which is a number that still allows a wide family of airfoils to be generated.

With R and Ω being the radius and the angular speed of the turbine and $q_\infty \exp(-i\alpha)$ the complex velocity of the wind, the complex potential $w(\zeta)$ can be written as

$$w = Q_\infty e^{-i\beta}\zeta + \frac{Q_\infty e^{i\beta}}{\zeta} + \frac{1}{2\pi i}\sum_{j=1}^{J}\gamma_j \log\frac{\zeta-\zeta_j}{\zeta-1/\bar{\zeta}_j} + \sum_{n=1}^{N}(a_n + ib_n)/\zeta^{n-1}$$

with $Q_\infty e^{-i\beta} = \lim_{\zeta\to\infty} q_\infty e^{-i\alpha} dz/d\zeta$ and γ_j, ζ_j being the circulation and location of the vortex singularities. The last term is a series, suitably truncated at a large value N, that takes into account the motion of the blade. The a_n, b_n coefficients can be derived by the value that the stream function has to hold on the blade contour in order to satisfy the impermeability condition (see, for instance, [11]). In fact, with $\zeta = \rho\exp(i\varphi)$, on the blade contour, where $\rho = 1$, the relationship

$$\Im[w(\zeta)] = \sum_{n=1}^{N} b_n \cos(n-1)\varphi - a_n \sin(n-1)\varphi = U\Im[z(\zeta)] - V\Re[z(\zeta)] - \frac{\Omega}{2}|z(\zeta)|^2 \qquad (1)$$

has to be satisfied, with U, V being the Cartesian components of the blade speed $q = R\Omega$.

A blob vortex method is used to model the vorticity shed by the blade edges. It is based on generating vortices at constant time intervals in $z(\zeta_{v_T})$ locations close to the $z(\zeta_{T_i})$ trailing edges. The circulation γ_{v_T} of the new born vortices is determined by satisfying the Kutta condition, that is, by enforcing the flow separation at the edges. For the moving blade here considered, this condition is expressed by the equations $\Im(\zeta dw/d\zeta)_{\zeta_{T_i}}$=0, with $T_i = T_1, T_2, T_e$. The new generated vortices increase the total number J of the vortices advected by the flow. The vortex trajectories are numerically computed by evaluating their velocity according to the Routh Rule (see, for instance, [12]).

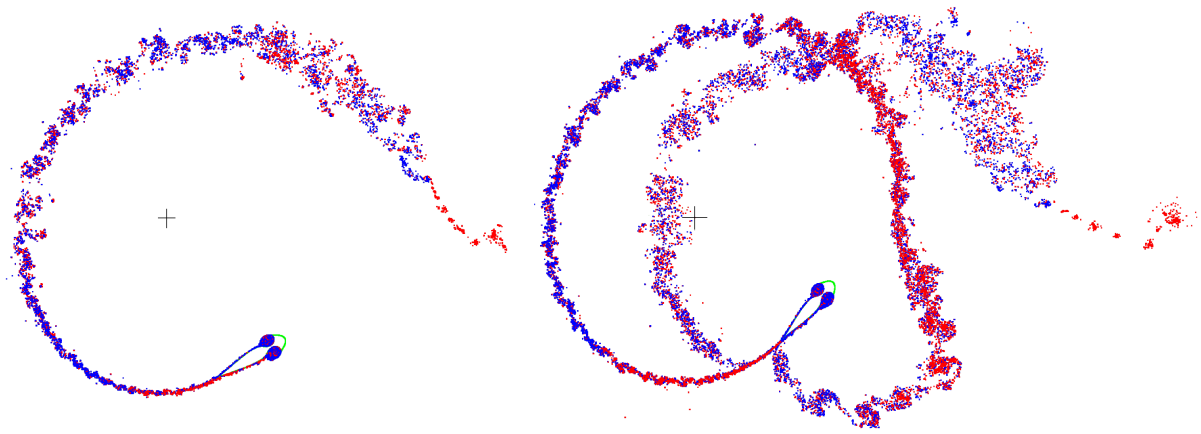

Figure 2. Flow visualization.

2.1. Numerical example

Fig. 2 shows snapshots of the visualization of the flow past a single blade turbine. The motion is impulsively started, it is pertinent to a turbine whose blade-chord to turbine-radius ratio is $l/R = 1/2$ and whose turbine-speed to wind-speed ratio is $\Omega R/q_\infty = 5$. The dots in the figure represent the shed vortices. The red ones are pertinent to counter-clockwise circulations, the blue ones to clockwise circulations.

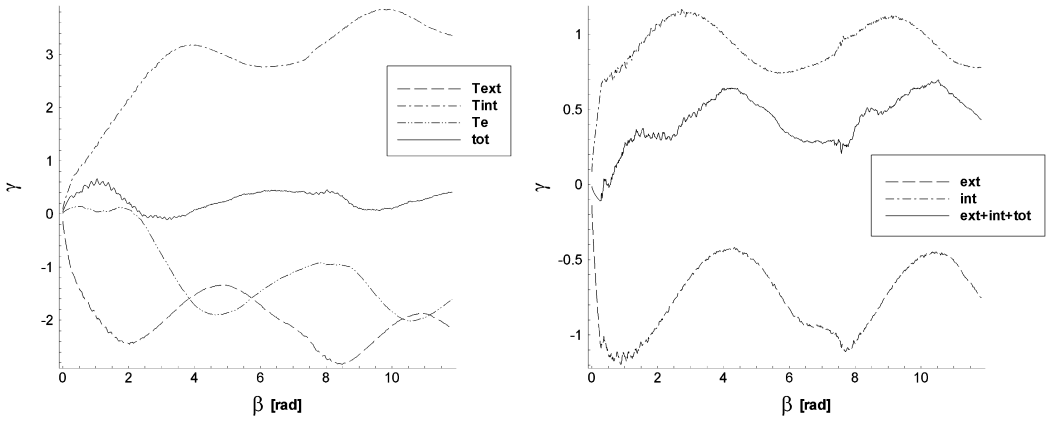

Figure 3. Circulation time history.

The time evolution of the vorticity shed by the airfoil edges is plotted on fig. 3. The time integral of the circulation shed by the internal, external and trailing edges and the blade circulation are plotted versus the blade rotation angle in the left-hand side of the figure . The circulation around the blade is equal and opposite to the sum of the circulations of the shed vortices. In spite of the symmetry of the angle of attack evaluated as the resultant of both the blade and wind speed, the blade circulation ends being periodic with a non null, positive average value. Indeed, the motion of the blade is circular, with the internal side of the blade differently acting from the external one; moreover, the flow is affected by the wake. The right-hand side of

the figure shows the time history of the circulations of the trapped vortices and the sum of the blade circulation and the trapped vortex circulations.

As long as the stall does not occur, the visualization of the flow past a traditional blade section should not be far from the present one. Indeed, though some advantage on the blade lift is expected by the trapped vortices, the main sought effect is the control of the stall, according to the mechanism briefly described in the introduction section.

3. Two blade turbine

In principle, the method used to study turbines with a single blade can be extended to turbines with any number of blades. In practice, such extension is not simple. The main difficulty consists in going from problems in simply connected domains to problems in multiply connected domains. A general way to treat flow problems in multiply connected domains has been recently suggested by Crowdy [13]. In the present work we prefer to restrict the problem to the case of a turbine with two blades. A rather classical solution, based on the use of elliptic functions, is feasible for this case.

The general idea is to map the doubly connected domain bounded by the blades onto a circular ring, where the flow complex velocity can be defined by means of elliptic functions. Ives [10] has provided a general procedure to solve the mapping problem. It is based on a mapping chain that uses a sequence of Kármán-Trefftz, Theodorsen-Garrick and Garrick transformations.

With the same spirit as in the study carried out for the single blade turbine, we simplify the mapping problem to speed up the flow computation with the minimal purpose of illustrating the trapping vortex mechanism. As well as for the single blade case, we devise a closed form mapping that generates a couple of Kármán-Trefftz-like airfoils from a circular ring.

The mapping sequence is shown in fig. 4. Let us consider the ring formed by the circles centered on the origin of the σ-plane and having the radii $L < 1$ and $1/L$, respectively. The Möbius mapping

$$\zeta = i\eta_o \frac{1+\sigma}{1-\sigma}$$

maps the two circles onto the two mirrored Apollonius circles c_u, c_d of the ζ-plane, which have the foci at $\zeta_o = \pm i\eta_o$, the centers at $\zeta_c = \pm\zeta_o(1+L^2)/(1-L^2)$ and the same radius $\rho_c = 2L\eta_o/(1-L^2)$. The ring is mapped onto the domain of the ζ-plane bounded by the two c_u, c_d circles in a way such that the region inside the unit circle of the σ-plane is mapped onto the positive-imaginary half-ζ-plane and the outside region onto the negative half-plane.

The function

$$\nu = \left[\zeta^2 + \frac{a}{\zeta^2-\zeta_1^2} + \frac{b}{\zeta^2-\zeta_2^2} + \frac{a}{\zeta_1^2} + \frac{b}{\zeta_2^2}\right]^{1/2}$$

maps the two circles onto the two figures of the ν-plane, which can be superimposed over one another by a π rotation. The meaning of the parameters is the same as in the single blade mapping; the a, b parameters are such that$(d\nu/d\zeta)_{\zeta_{T_1}} = (d\nu/d\zeta)_{\zeta_{T_2}} = 0$, as well. Finally, the mapping

$$\frac{z^2 - z_{T_e}^2}{z^2 - z_N^2} = \left(\frac{\nu^2 - \nu_{T_e}^2}{\nu^2 - \nu_N^2}\right)^\tau, \qquad \tau = 2 - \epsilon/\pi,$$

generates the two blades on the physical z-plane. The values of z_{T_e}, z_N are defined by the conditions $z(0) = 0$ and $\lim_{\nu\to\infty} dz/d\nu = 1$, that is,

$$z_{T_e}^2 = \tau\,\nu_{T_e}^2 \frac{1-(\nu_N/\nu_{T_e})^2}{1-(\nu_N/\nu_{T_e})^{2\tau}}, \qquad z_N^2 = [z_{T_e}(\nu_N/\nu_{T_e})^\tau]^2\,.$$

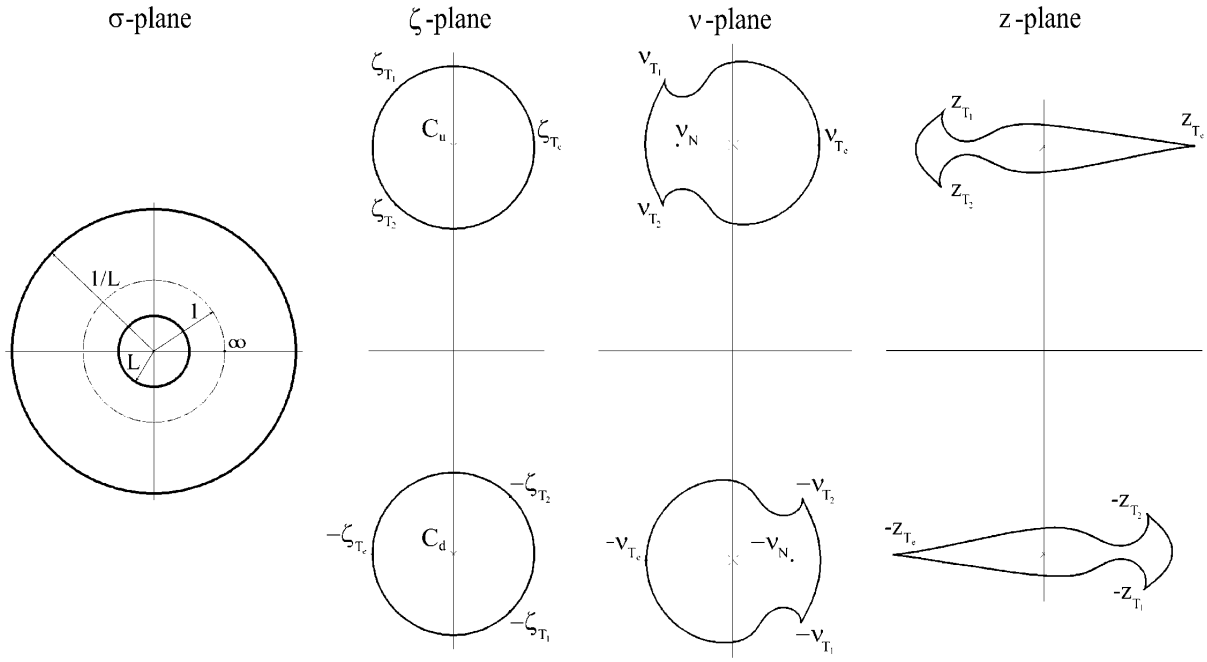

Figure 4. Mapping sequence.

To define the complex potential, it is convenient to map the ring of the σ-plane onto a rectangle of the further λ-plane by taking $\lambda = \log\sigma$. The edges of the rectangle are at $\lambda = \pm\log L \pm i\pi$, with the two circles mapped on the sides $\Re(\lambda) = \pm\log L$. We first consider the turbine as standing at rest; the stream function is constant on the blades and, as a consequence of the infinite number of reflections on the rectangle sides, the complex velocity is expressed by a doubly periodic function on the λ-plane, whose semi-periods are $\omega = -2\log L$ and $\omega' = i\pi$. This function must have a second order pole to represent the wind velocity and first order poles to represent the vortex singularities. It can be built by means of the $\wp$, ζ and σ Weierstrass elliptic functions as:

$$\frac{dw_{rest}}{d\lambda} = M\wp(\lambda) - \bar{M}\wp(\lambda+\omega) + \frac{1}{2\pi i}\sum_{j=1}^{J}\gamma_j[\zeta(\lambda-\lambda_j) - \zeta(\lambda+\bar{\lambda}_j-\omega)] + i\kappa,$$

whose integration yields

$$w_{rest} = -M\zeta(\lambda) + \bar{M}\zeta(\lambda+\omega) + \frac{1}{2\pi i}\sum_{j=1}^{J}\gamma_j\log\frac{\sigma(\lambda-\lambda_j)}{\sigma(\lambda+\bar{\lambda}_j-\omega)} + i\kappa\lambda,$$

with $\lambda_\infty = \lim_{z\to\infty}\lambda(z) = 0$. The M, κ parameters are defined by the conditions that flow velocity at infinity is the wind velocity, that is, $\lim_{\lambda\to\lambda_\infty}(dw_{rest}/d\lambda) = q_\infty\exp(-i\alpha)$ and by enforcing the condition that there is no circulation at infinity, that is, that for $\gamma_j = 0$ the blade circulation has to be null, which yields

$$\Re\{[-M\zeta(i\omega') + \bar{M}\zeta(i\omega'+\omega)] - [-M\zeta(-i\omega') + \bar{M}\zeta(-i\omega'+\omega)] - 2\kappa\omega'\} = 0.$$

The complex potential for the moving blades can be written on the σ-plane as

$$w = w_{rest}(\log\sigma) + \sum_{n=1}^{N}(a_n + ib_n)(L\sigma)^{n-1} + \sum_{n=1}^{N}(c_n + id_n)(\sigma/L)^{-(n-1)},$$

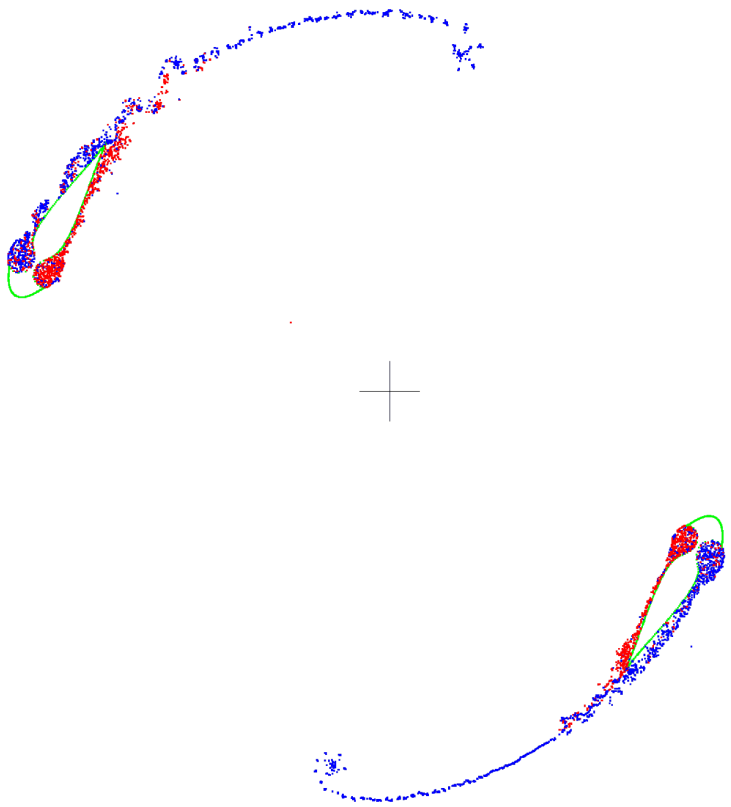

Figure 5. Starting flow of a two-bladed turbine.

where the coefficient of the two series can be obtained by enforcing the values that the stream function has to attain on the blades to satisfy the condition of impermeability. By considering that the axis of the turbine is located on the origin of the z-plane, these are:

$$\psi_u = -\frac{\Omega}{2}|z(e^{i\varphi}/L))|^2, \qquad \psi_d = -\frac{\Omega}{2}|z(Le^{i\varphi}))|^2,$$

where φ is the anomaly on the σ-plane. The following two relationships can be hence derived:

$$\psi_u = \sum_{n=1}^{N}(b_n + d_n L^{2n-2})\cos(n-1)\varphi + (a_n - c_n L^{2n-2})\sin(n-1)\varphi,$$

$$\psi_d = \sum_{n=1}^{N}(b_n L^{2n-2} + d_n)\cos(n-1)\varphi + (a_n L^{2n-2} - c_n)\sin(n-1)\varphi.$$

Thus the coefficients a_n, b_n, c_n, d_n can be evaluated.
As well as it has been described for the single blade case, the vortex method is implemented to describe the shedding of vorticity from the six edges of the two blades. The Kutta condition can again be written as $\Im[\exp(i\varphi)dw/d\sigma] = 0$ at the six edges. Therefore, the circulation of the new shed vortices can be computed.

3.1. Numerical example
An example of the flow past a two-bladed turbine is shown in fig. 5. The flow is visualized during the initial transient of the impulsively started motion. Vorticity is shed by the edges of the blades, vortices are going to be trapped by the cavities and typical starting vortices are shed by the trailing edges into the wake. As well as for the flow pertinent to a one-bladed turbine, the red dots are relevant to a positive circulation and the blue ones are relevant to a negative circulation.

4. Evaluation of the performances

The rigorous evaluation of the lift and torque from the results as given by the blob vortex method is not a simple and straightforward task. In fact, it consists on finding the dynamical effects of a rotational unsteady incompressible flow on a multiply connected domain with moving boundaries. There are two main methods that can be considered. One consists on determining the pressure on the body contours by means of the unsteady Bernoulli equation. The generalized Blasius formulas, as described in [11] could be used to this purpose. The other method consists on determining the forces as time derivatives of the impulse, as discussed, for instance, by Saffman [15] and references therein.

With the first method the pressure is to be determined on the body walls. Unfortunately, it is unsuitable for vortex methods for the strong noise that affects the pressure signal at the walls as a consequence of the vorticity concentrated by the vortex method.

The second method to compute the dynamical actions is more suitable to the present flow simulation and it is the way that we intend to follow. For moving boundaries in a multiply connected region and with bodies having circulation, there are still open problems to be faced. Recent contributions can be found in the literature about such issue. See, for instance, [15],[16],[17],[18],[19] and references therein. Such a subject goes behind the scope of the present work and it deserves a dedicated study.

The use of different approaches, which would allow for a simpler force evaluation, is discouraged by considering that vortex methods are the best suited methods for describing turbulent unsteady motion affected by vortex shedding. RANS simulations, especially when the flow is unsteady, quite often are unreliable; LES should be much more reliable, but the computational effort would be much greater.

As final consideration, a rough approximation of the forces could be attempted by assuming the flow as quasi-steady, that is, by applying the Joukowski theorem to the instantaneous blade circulation as due to the instantaneous asymptotic relative velocity assumed as steady. As below discussed, this approach also is illusory. In fig. 6 the actual blade and trapped vortex circulation (solid line), as computed by the vortex method, is compared to the circulations the blade would experience if the flow were steady. The dot line is pertinent to a blade with trapped vortices, while the dot-dash line refers to a blade without trapped vortices. The actual unsteady circulation is very far from the steady ones and it does not allow for a realistic approximation of the performances on the basis of a quasi-steady approximation; it shows a much smaller amplitude and a different phase as a consequence of the transient nature of the flow and of the wake effect.

The steady circulation past the blade with trapped vortices has been computed analytically by enforcing the Kutta condition at the three edges of the blade for a given relative velocity at infinity. It allows to compute the circulation at infinity and the strength of the trapped vortices, which are assumed as point vortices located in equilibrium position. The vortex equilibria result as being stable. The method used to determine the equilibrium locations of the trapped vortices and their stability is described in [6].

The comparison between the steady circulations offers a clue on the effect of the trapped vortices. The amplitude of the circulation pertinent to the blade with trapped vortices is

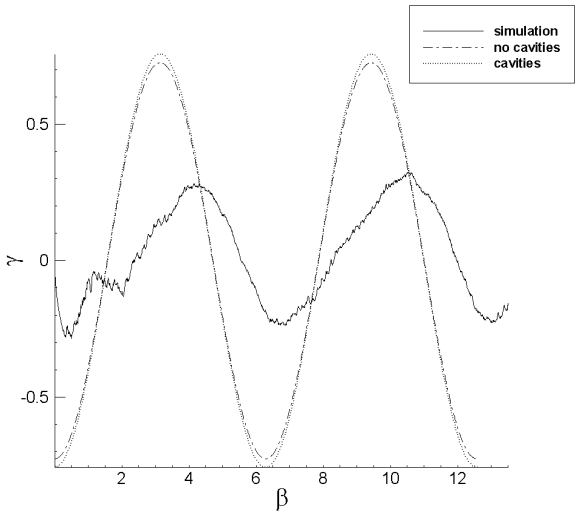

Figure 6. Steady and unsteady single blade circulations ($\Omega R/q_\infty = 5$).

slightly greater than the amplitude without trapped vortices, the effect of enhancing the turbine performances should be small. Indeed, as remarked in Sec. 2.1, the main outcome expected by the trapped vortices is the stall control rather than the performance enhancing, which however is present.

5. Conclusion

The flow past a one bladed and a two bladed vertical axis turbine has been computed by means of an analytical-numerical method. The blade profiles have been generated analytically; they have cavities suited to trap vortices. The numerical examples show that vortical structures are generated and trapped by the cavities and that vortex shedding is prevented. This result has been obtained in the limit of an inviscid model and does not take into account the possible local occurrence of secondary separations. Nevertheless, the result is meaningful for two main reasons: firstly, inviscid vortex methods, as the one here adopted, are able to describe the vortex shedding phenomena past bluff bodies, with the correct Strouhal number (see, for instance, [14] and therein references). In fact, the Kutta condition models the main viscous effect causing flow separation, then inertia rather than viscosity governs the global instability of the vortex shedding phenomena. Secondly, the instability that is triggered by secondary separations due to local adverse pressure gradients has a characteristic relaxation time. If this time is greater than the turbine period the instability could be not triggered.
The present study is in progress. Next steps will provide the evaluation of the torque and a conformal mapping method for arbitrary blade sections.

[1] Ringleb F. O. 1961. Separation control by trapped vortices. In: Boundary Layer and Flow Control, Pergamon.
[2] Iollo A., Zannetti L. 2001. Trapped Vortex Optimal Control by Suction and Blowing at the Wall. Eur. J. Mech./Fluid, 20, pp7-24.
[3] Chernyshenko S.I., Galletti B., Iollo a., Zannetti L. 2003. Trapped Vortices and a Favorable Pressure Gradient. J. Fluid Mech., 482, pp. 235-255.
[4] Zannetti L., Chernyshenko S.I. 2005. Vortex Pair and Chaplygin Cusps. Eur. J. Mech./Fluid, 24, pp. 328-337.
[5] Galletti B., Iollo A., Zannetti L. 2002. Aerodynamic Constraints for Vortex Trapping Airfoils. Acc. Sc. Torino - Atti Sc. Fis. 136 (2002), pp 21-30.
[6] Zannetti L. 2006. Vortex equilibrium in flows past bluff bodies. J. Fluid. Mech. 562, pp. 151-171.

[7] VCell2050. http://www.vortexcell2050.org/.
[8] P. Deglaire, O. Ågren, H. Bernhoff, M. Leijon 2007. Conformal mapping and efficient boundary element method without boundary elements for fast vortex particle simulations. Eur. J. Mech. B/Fluids, doi:10.1016/j.euromechflu.2007.03.005
[9] Moretti G. 1980. Grid generation using classical techniques. Workshop on Numerical Grid Generation Techniques for Partial Differential Equations, Oct. 1980. ICASE, NASA Langley Research Center.
[10] D.C. Ives 1976. A modern look at conformal mapping, including multiply connected regions, AIAA J. 14 (1976) 10061011.
[11] Milne-Thomson L.M.1968. Theoretical Hydrodynamics. Dover 1996.
[12] Clements R. R. 1973. An inviscid model of two-dimensional vortex shedding. J. Fluid Mech, 57, pp. 321-336.
[13] Crowdy D.G. 2006, Analytical solutions for uniform potential flow past multiple cylinders. Eur. J. Mech./Fluid, 25, pp 459-470.
[14] Zannetti L., Iollo A. 2003. Passive Control of the Vortex Wake Past a Flat Plate at Incidence. Theoret. Comput. Fluid Dyn. 16: 211230
[15] Saffman P.G. 1992, Vortex Dynamics, Cambridge University Press, NY.
[16] Biesheuvel A, Hagmeijer R On the force on a body moving in a fluid. Fluid dyn. res. 38 (10): 716-742 OCT 2006
[17] Pan LS, Chew YT A general formula for calculating forces on a 2-D arbitrary body in incompressible flow. J. Fluids and Structures 16 (1): 71-82 JAN 2002
[18] Protas B., On an Attempt to Simplify the Quartapelle-Napolitano Approach to Computation of Hydrodynamic Forces in Open Flows. Journal of Fluids and Structures (accepted for publication), 2007
[19] Wells J.C. Calculating the impulse and angular impulse of image vorticity by integrals over free vorticity. Proc. R. Soc. Lond A - (1998) 454,2791-2809